THE ELECTROCHEMICAL ETCHING PROCESS OF A TUNGSTEN WIRE

Aaron M. Richardson, B.S.

Thesis Prepared for the Degree of

MASTER OF SCIENCE

UNIVERSITY OF NORTH TEXAS

August 2021

APPROVED:

Duncan Weathers, Major Professor
Jose Perez, Committee Member
David Shiner, Committee Member
Jingbiao Cui, Chair of the Department of Physics
Pamela Padilla, Dean of the College of Science
Victor Prybutok, Dean of the Toulouse Graduate School

Richardson, Aaron M. *The Electrochemical Etching Process of a Tungsten Wire.* Master of Science (Physics), August 2021, 30 pp., 2 tables, 14 figures, 1 appendix, 8 numbered references.

This study produced and analyzed shaped tungsten wire tips formed through electrochemical etching. Specifically, the cone length and the radius of curvature of the tip were analyzed. Having the tips move dynamically through an electrolytic solution, such as potassium hydroxide, and tuning the initial starting depth of the tungsten wire along with the dynamic speed of the tungsten wire as it passed throughout the solution allowed various types of tip profiles to be produced. The tip's radius of curvature was able to be reproduced with an accuracy between 88 - 92 %. The method provided would be applicable for the production of various styles of liquid-metal ion source (LMIS) probes and scanning probe microscope (SPM) tips.

ACKNOWLEDGEMENTS

I would like to acknowledge and express my thanks to all those who had led me to where I am today. First, I would like to thank my advisor/research leader, Dr. Duncan Weathers. His enthusiasm and passion for physics has been inspirational to me, and I grateful for that. Next, I would like to thank my committee for taking their time to support me: Dr. Duncan Weathers, Dr. Jose Perez, and Dr. David Shiner. After that, I would like to thank the UNT Physics Department and faculty. They have been able to share a vast amount of knowledge and experience related to many fields in physics, and I am very grateful for all the opportunities that I have been given. Finally, I would like to thank my friends and family. They have been there for me when times were challenging, and when I needed to vent about any type of nonsense. I am very thankful to have everyone of these people in my life.

TABLE OF CONTENTS

Page

LIST OF TABLES AND FIGURES

Page

Tables

Figures

CHAPTER 1

INTRODUCTION

1.1 History

Etching has been a known trade for many centuries. It dates back as far as the early 15th century when etching was originally used to create artwork onto armor plates and sword handles by using strong acids or mordants. It was used far more due to how simple it was, rather than the more difficult engraving of armor plates. Daniel Hopfer (1470-1536), a German artist, was well known for his decorated armor and shields, which can still be viewed in museums today. During today's age, etching is still used for artwork, but it is now a technique that is used to create complex circuit boards, or to etch various grades of wire into needle-like shapes.

1.2 Real World Applications

Various types of scanning probe microscopy (SPM), such as the scanning transmission electron microscope (STEM), the field emission scanning electron microscope (FESEM), and the scanning tunneling microscopy (STM), all use electrochemically etched tips. These instruments are used to study the structure of nanoscale material. These probes are commonly formed from tungsten due to its tensile strength. It can provide high resolution images by having the tungsten needle scan across the surface of the sample being studied. Sharp tips consisting of a small radius of curvature with a low taper angle (steep concavity in shape) will provide high image quality while scanning the surface [2,4,5,6].

Tungsten wire can be etched into cone-shaped probes that can be utilized for the study and application of liquid-metal ion sources (LMIS). The use of tungsten as a probe allows

studies needed to be conducted at high emission currents (several milliamperes) [3]. Cones that consist on a convex shape with a small radius of curvature will be able to perform well in the experiments. The preferred surface texture of these tips would be a rough surface [1,4,8].

1.3 Background Information

Being able to study the effects that electrochemical etching has on a tungsten wire will allow methods to be used to etch suitable tips for applications. Figure 1.1 introduces the dynamic method approach, where the wire is continuously moving throughout the solution.

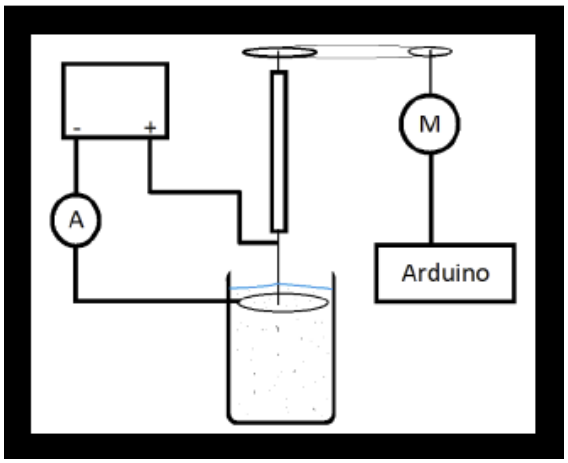

Figure 1.1: Basic electrochemical etching process setup.

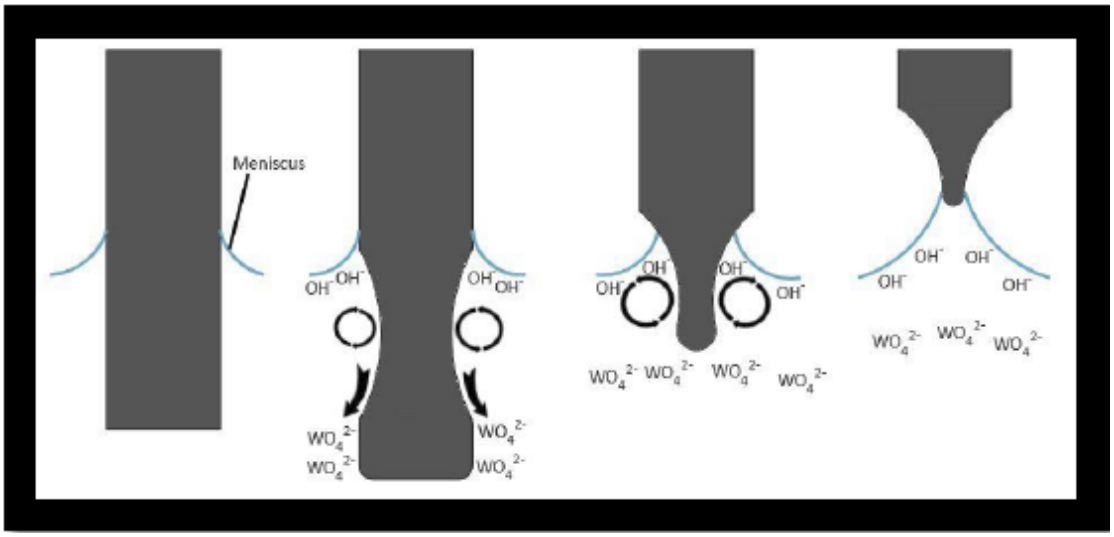

Figure 1.2: Four-step diagram of the etching process.

Figure 1.1 gives the basic setup for electrochemical etching. This setup depicts the use of a stepping motor plunging a wire into a beaker filled with an electrolytic solution. The electrochemical etching process begins by applying a voltage to the etching apparatus. This voltage is provided from our electric etching controller to our submerged tungsten (W) wire. The tungsten wire acts as the anode, while a stainless-steel pipe is used as the cathode. Centering the anode in the aqueous solution inside the cathode will produce a uniform electric field in the system [2]. The cathode is then connected back into the etching controller. Our aqueous solution housing the two is of a commonly used electrolyte, potassium hydroxide (KOH) [2,7]. During the etching process an anodic dissolution will occur, where the tungsten will begin to shed off the outer layers of its surface into soluble tungstate anions, WO_4^{2-} [7]. The chemical reaction for the anode is as follows:

$$W(s) + 8OH^- \rightarrow WO_4^{2-} + 4H_2O + 6e^- \quad \text{(Eq. 1.1)}$$

with a standard oxidation potential (SOP) of 1.05 V for tungsten. The stainless-steel pipe will begin to give off hydrogen gas bubbles and OH^- ions. The chemical reaction for the cathode is as follows:

$$6H_2O + 6e^- \rightarrow 3H_2(g) + 6OH^- \quad \text{(Eq. 1.2)}$$

with a standard reduction potential (SRP) of -2.48 V for water. The overall chemical reaction is then:

$$W(s) + 2OH^- + 2H_2O \rightarrow WO_4^{2-} + 3H_2(g) \quad \text{(Eq. 1.3)}$$

The standard electrode potential, E^0, will be the sum of the SOP and SRP voltages. To produce the tungstate anions, the applied electrical potential will need to be set to a voltage greater than E^0.

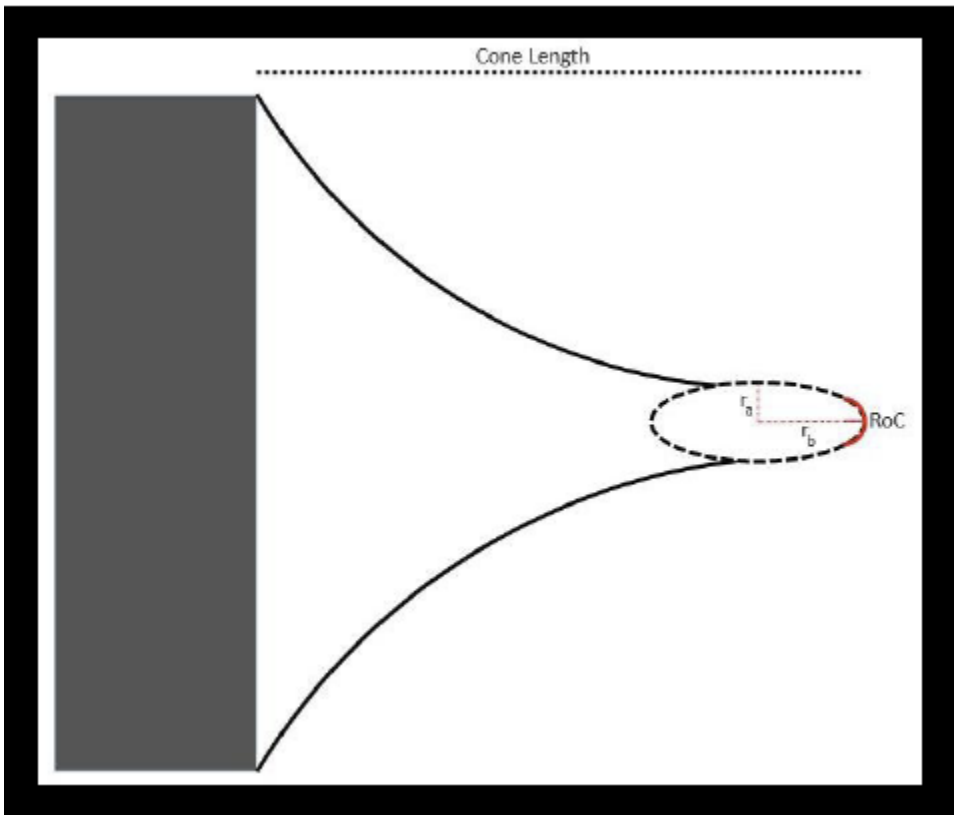

Figure 1.3: Diagram of the tungsten needle profile.

At the surface of the solution, a meniscus is formed around the inserted tungsten wire. The meniscus is the most important part in shaping the features of the tungsten needle [2]. It will travel 0.367 mm up the tungsten wire when the wire makes initial contact with the solution. There will be a buildup of OH^- ions in the top layer of the solution, based on the information given in equation 1.2. These ions will repulse the WO_4^{2-} anions down the inserted tungsten wire and will act as a barrier. This anodic flow will create a vortex within this barrier and will be where the etching rate is at its strongest. A common term for the action taking place in this region is “necking” [2,7]. This is when the wire is thinning out due to the dissolution of the tungsten into tungstate. Etching is completed when the circuit opens. An open circuit can be obtained when the tensile strain in the necking region becomes too great and the wire snaps

into two halves [6]. Another way to open the circuit is to remove the anode from the solution. The final resulting look for the etched wire will be conical. The cone's profile can vary by altering simple variables. The surface texture of the cone can be altered; if a rough surface is desired, then etching at a low voltage of 2 V will do. An increase in the voltage will increase the smoothness of the cone's surface. The roughening of the surface is commonly referred to as "roughing" [4]. The tip profile can be concaved in shape, or as depicted in Figure 1.3, can have a complex shape. This shape can also be defined as the taper angle [4].

CHAPTER 2

ETCHING OVER TIME

2.1 Objectives

It has been stated that the depth of the cathode will affect the length of the inserted wire; the lower the cathode is placed then the longer the probe can be [6]. This makes sense because this would deepen the barrier of the etching vortex. The focus of this part of the study was a shift in the results published by Bing-Feng Ju to determining how the initial depth of the wire will alter the length of the needle. Learning the effects that depth has will allow further studies to be conducted, which will increase the understanding the electrochemical process happening to the wire.

2.2 Equipment and Parameters

Tungsten wire was cut from a spool of tungsten, where the diameter of the wire was 0.25 mm. An 80 mL beaker filled with distilled water was used to mix and hold the KOH solution. The amount of KOH pellets measured was 4.4884 grams. This produced a molar concentration of 1.

An etching controller, which was made by the UNT Physics Department's electronics shop, was used to supply the electric potential in the closed system. It was connected from a 120 V AC wall outlet and supplied 10 volts through an alligator clip clipped to a copper wire [8]. The copper wire was fitted to the threads of the screw holding the tungsten wire in place. This is how the wire became the anode of the system. Another alligator clip traveled from the etching controller to a stainless-steel pipe. This pipe was then inserted into the 1 molar concentration of KOH solution. To complete the circuit, the solution was slid under the wire,

and the wire was lowered to its zeroed level (the initial insertion position of the wire into the solution).

An Arduino UNO R3 controlled a NEMA 17 stepping motor, which was used to turn a micrometer to plunge the needle in and out of the solution. This Arduino was programmed to control the dynamic speed at which the wire passed into the solution. This was one of two methods (static and dynamic) used to control the outcome of the tungsten needle's profile [6]. The program, created from Arduino IDE, consists of a series of if-else statements that give power to certain pins on the stepping motor controller chip, causing the motor to step and the wire to move. A double-pole single-throw switch controlled the output signals from the Arduino to the pins, where the neutral position stopped the needle from moving, while the other positions controlled either the forward direction (plunging into the solution) or the reverse direction (reversed from the solution). The chip used to control the motor was a TB6612 manufactured by Adafruit. Gears and a chain were connected from the stepping motor to the micrometer that controlled and determined the depth of the wire.

The micrometer that was connected to the stepping motor held the tungsten wire in the mechanical setup. The micrometer needed to be placed at various levels to accommodate the needed initial depth of the wire. Having the micrometer starting at 0 mm was not ideal due to the gears that connected the micrometer to the stepping motor. This would have caused the chain to slip and would interrupt the movement of the wire as it passed into the solution. The same results would follow if the micrometer reached its limit of travel.

The tool used to image each needle was a microscope and digital camera connected to PAX-it! software. A clear and clean image could be taken, and the software offers tools that

could be used to determine many aspects of the image. The tools used with this setup in this experiment were the image capture and image measure tools.

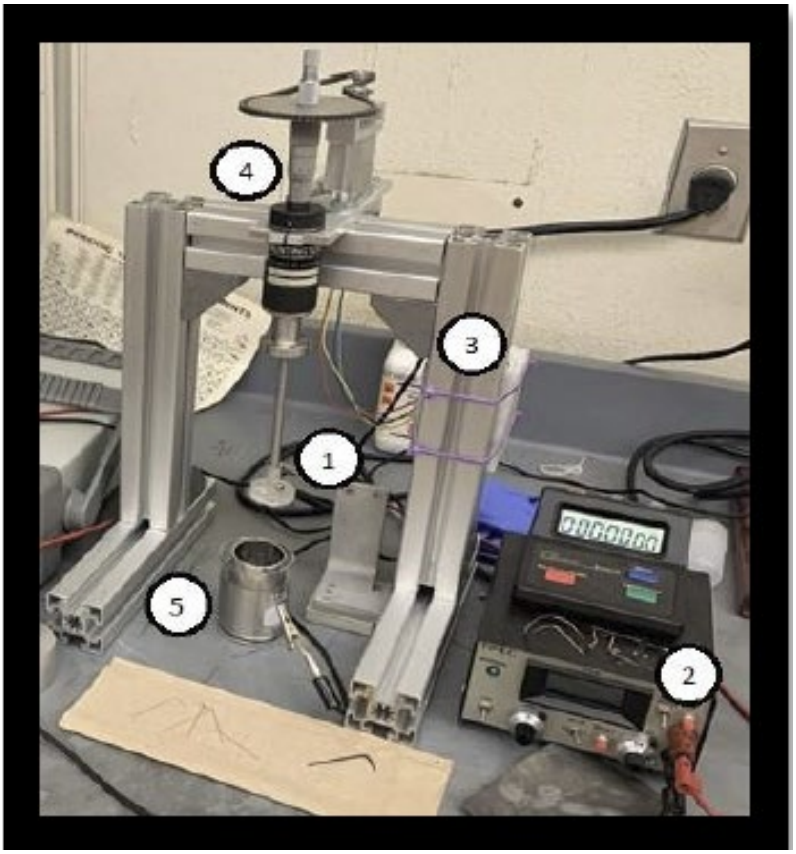

Figure 2.1: Electrochemical etching system setup.

(1) Tungsten wire and test-rig; (2) etching controller; (3) Arduino board circuit and the stepping motor (attached to the back of the post); (4) micrometer; and (5) electrolyte solution and stainless-steel pipe.

2.3 Data Taking Procedures

The zero level of the tungsten wire was recorded. The zero level corresponds to when the wire first contacted the surface of the solution. The solution then traveled up the wire approximately 0.367 mm, creating a meniscus around the wire. The distance was recorded in increments of 2 minutes for 15 minutes as the wire traveled down into the solution. Then the movement of the needle was reversed until the etching was completed, while the distance is recorded in increments of 2 minutes. As the wire was being etched, the current was recorded

throughout the process. The newly etched tungsten needle than looked like a cone. The microscope was used to view each needle and the PAX-it! software was used to measure the cone's length, which was recorded.

2.4 General Procedures

5 cm of tungsten wire was cut off from the spool of tungsten. Sanding the snipped edge with P-280 grade sandpaper gave the wire a flat end without damaging the needle any further. If not sanded the wire's final etch would be disfigured. One cm of the wire was bent to create a "foot"; which was what held the wire in place on the test-rig. The wire was secured in place by twisting a screw until a "snug-fit" was reached. This ensured that the wire stayed in place without damaging the wire.

Next the etching solution was mixed: KOH at a concentration of 1 mole. Cleaning the equipment was important. This was to ensure that the solution stayed as pure as possible. Placing a total of 4.4884 grams of KOH pellets into 80 mL of deionized water obtained the 1 molar concentration. Increasing the molarity would also increase the etching speed. The total gram atomic mass of KOH is 56.1 grams, and using the following equation allows one to manipulate the solution:

$$mol\ solute = Molarity * L\ of\ solution \quad \text{(Eq. 3.1)}$$

$$mass\ of\ KOH = mol\ solute * gram\ atomic\ mass\ of\ KOH \quad \text{(Eq. 3.2)}$$

where L is the amount of solution in liters, the molarity was equal to 1, and the gram atomic mass of the KOH pellets is 56.1 grams per mole. Stirring the pellets into the deionized water assisted in dissolving the KOH. The solution was mixed until the solution turned transparent.

The test-rig was connected to the positive output of the etching controller. This made

the wire into an anode, while a stainless-steel cylinder pipe placed in the solution acted as the cathode. The test-rig was next connected, with a screw, to the etching setup. The solution was placed under the test-rig. The solution was aligned so that the wire was centered in the pipe. The needle was lowered to its zero level, then, if needed, to its desired depth into the solution by manipulating the micrometer dial.

Next, the etching controller was turned on. This instrument allows a set voltage to be applied to the wire. The desired voltage was 10 V. The etching controller has a feature allowing the etching current to be monitored while the voltage is being applied. Monitoring the current informed the observer of any irregularities going on during the etching process.

The Arduino was then activated. The program permitted the needle to plunge in then out of the solution. This plunging process could be modified. The delay within the stepping motor was specifically manipulated to increase or decrease the wire's speed as it passed into the solution. This modification was referred to as the delay speed of the wire. A total of up to 30 minutes was used to etch the wires into needles: 15 minutes for the wire to plunge into the solution, then a maximum of 15 minutes (or shorter if the process ended before then) for the wire to be drawn out from the solution.

Finally, imaging the needle samples could be done. The needles were very delicate, and therefore any rough movement across the needle tip could damage the cone. The needle was placed under a microscope and a Keim-wipe was used to clean any debris from the etching process. The magnification was set to 5x and displayed the image using PAX-it!; measurements of the cone profile could then be taken. Having a solid white background helped with determining the length to a point of accuracy.

2.5 Results

Figure 2.2: Tip profiles with varied initial depths and delay speeds.

Results gathered from tungsten wires which had varied initial depths and delay speeds. As the wire made initial contact, it was withdrawn either 0.1 mm, 0.2 mm, or 0.3 mm from the solution. The speed at which the motor stepped was delayed by a factor of 0.90, 0.95, and 1.0.

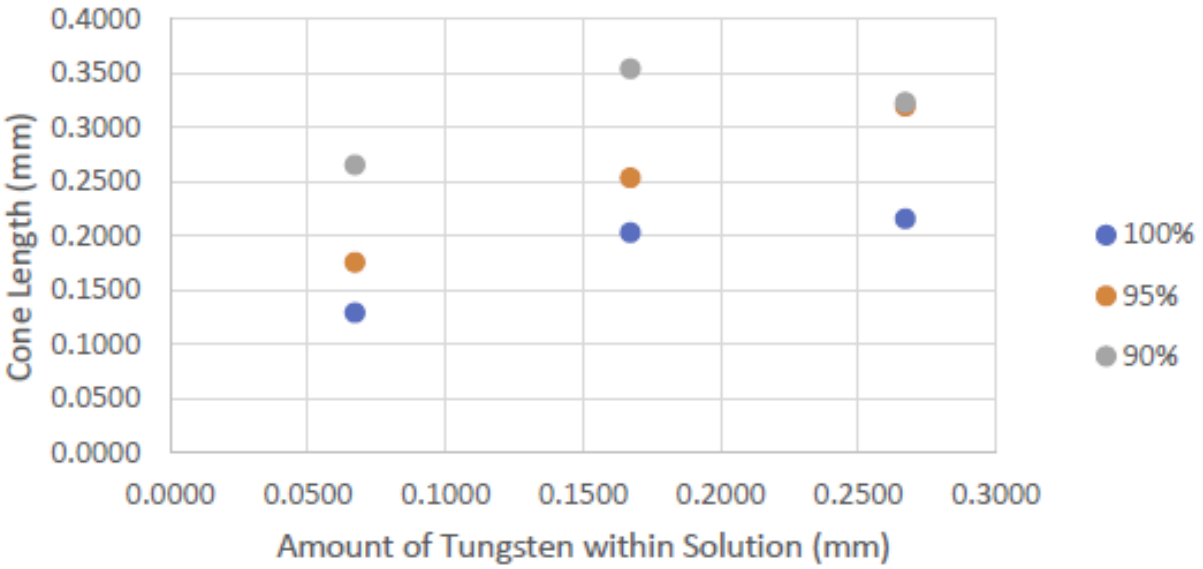

Figure 2.3: Stepping motor dealy speed at varied depths.

Varied initial depths the tungsten wire inserted into the solution versus the final length of the cone. Each depth was done at three different delay speeds.

The length of the cone was determined by using the PAX-it! software. A tool is provided where the initial point and final point could be measured, after being correctly calibrated. Each cone was measured against a ruler in millimeters, as seen in Figure 2.1.

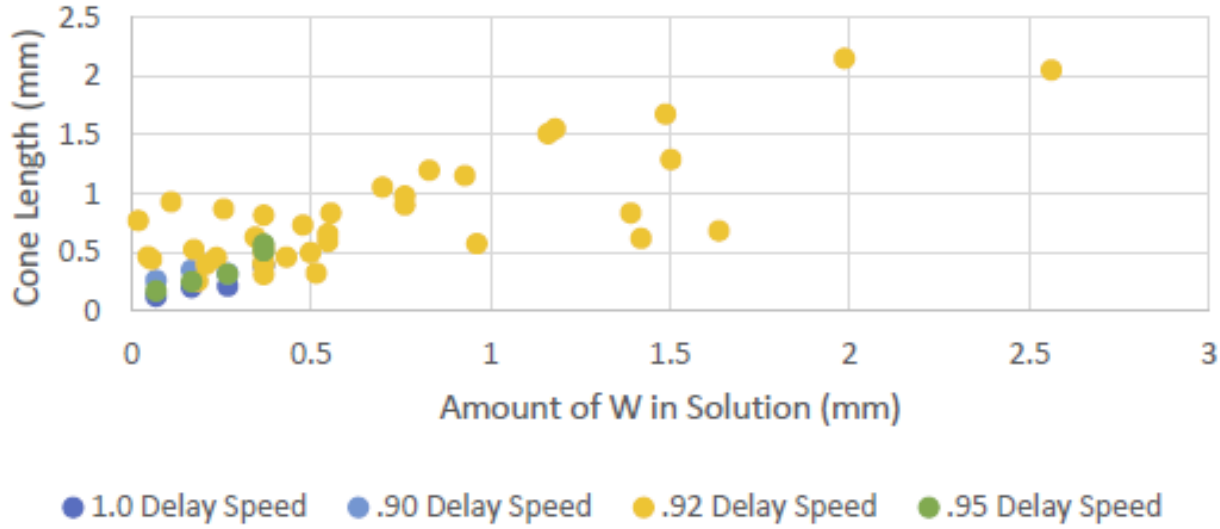

Figure 2.4: Cone length vs. amount of tungsten under solution with delay speeds.

This graph represents the final cone length at different initial depths. The delay between each step that the motor made as the wire passed into the solution varied from a factor of 0.90-1.0 during the trials.

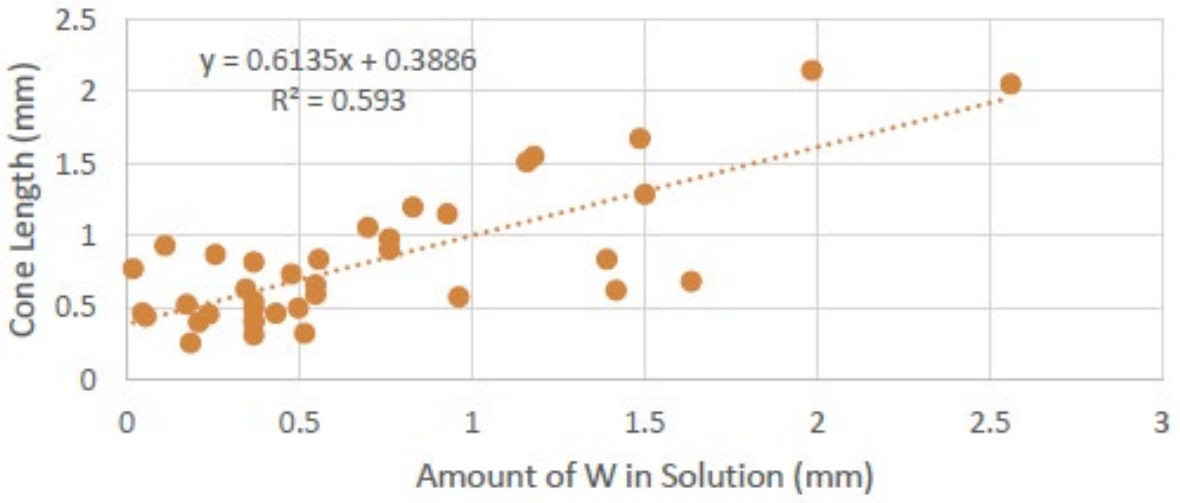

Figure 2.5: Cone length vs. amount of tungsten under solution at 0.92 delay speed.

This graph represents the final cone length at varied initial depths. The delay speed of the plunge was scaled by 0.92 during these runs.

2.6 Discussion

The cone length was affected by the amount of tungsten initially in the solution. The trend, as presented in Figures 2.4 and 2.5, was that as one increased the starting depth of the wire, then the resulting cone would be of greater length as well. This means that the needle's profile will change as the initial depth is varied. The etching process at deep depths (when the initial wire depth exceeds the etching barrier) snapped the tungsten within the solution. This was due to the anodic flow that traveled down the inserted wire, greatly decreasing the effects of the etching as shown in Figure 1.2. The requirement for a SPM tip would be realized at deeper depths, since the tips require a long, skinny, and sharp profile. The requirement for LMIS probes is better achieved at shallow depths. The speed at which the needle passed into the solution caused the cone length to vary as well. Allowing the needle to stay in the solution longer resulted in a continued etch. This is evident by looking at Figure 2.2, where one can see that for decreased speeds the taper angle of the cone become large. As the motor speed was

increased for a set of tungsten wires, the resulting cone length was greater than for a wire that traveled through the solution with a slower stepping rate, as can be seen by looking at Figure 2.3. This is true because if the wire stayed within the etching barriers, the surface area of the tungsten wire would dissolve itself into tungstate. This means the taper angle would begin to decrease, and the needle would begin to look long and skinny. Investigating further into Figure 2.3 there is a random anomaly for the tip 1a that could have occurred due to the amount of OH^- ions collected at the surface. Sometimes a cone's profile would look like a duck bill shape, but this was due to the wire having a tear at the tip from where the wire cutters made their snip, and that was not successfully sanded down.

There is an asymmetric shape to each tip. The vibration in the system from when the motor took a step could be the reason for the asymmetrical cone profile on each needle. As the needle vibrated a spike in the current was observed. This affected the time it took for a needle to be etched from the wire. As the motor stepped the wire would vibrate within the solution, which altered the meniscus of the tungsten. The asymmetry follows the shape of an ellipse. As the wire is rotated, the needle profile varies. This error seems to have no effect on the average cone length.

2.7 Conclusion

It was observed that the amount of time the tip spent in the solution altered its length. A multitude of depths ranging from 0 mm to 3 mm for initial starting depth were used. Altering the speeds for different runs was also done.

The cone's asymmetric profile can be adjusted by decreasing the amount of vibration in the system. Decreasing the stepping of the motor would provide a smoother movement down into the solution.

CHAPTER 3

MAPPING THE CURVATURE

3.1 Objectives

The focus of this part of the study was to monitor the etching process in more detail and to measure the reproducibility of various outcomes such as the curvature at the apex of the cone for repeated trials. A secondary focus was to be able to determine the length of the etched tungsten wire and successfully replicate the process. Being able to replicate the length would be the start of understanding the electrochemical process happening to the wire.

3.2 Equipment and Parameters

The setup was similar to that of the previous chapter with a few updates to the following parts: the chip controlling the motor, the cathode, and the code programming the Arduino UNO R3. A new feature that was added was the use of KI Tools (software used in conjunction with a Keithley Instruments ammeter) to monitor the current. This was added in series with the cathode and anode.

The new driver chip that replaced the TB6612 was the DRV8825, which was manufactured by Texas Instruments. This enabled a 1/32-step feature that smoothed the stepping of the NEMA 17 Motor, which minimized the vibration in the system. With this new chip, the code was altered but the process still followed the same commands as before.

The new cathode was cut from a pipe to the length of 5 mm. It was read that the depth of the cathode can affect the length of the etched cone. The further down into the solution the cathode is, the longer the cone becomes. The etching process increases when the cathode is partly above the solution level. In the experiment the cathode was placed just under the

surface of the solution.

Having the current measured by KI Tools afforded detailed information to help in understanding the current's part in the etching process. To setup KI Tools to monitor the current, the cathode and anode of the setup were connected to a current monitor in series. The current monitor connected to the computer running the program via USB. The trigger intervals were set to 1000 milliseconds for a maximum reading of 2000 triggers. This allowed shallow etching to process fully, which took around 30 minutes (1800 triggers). The results of the current recorded during the process were then exported to a .csv file used in Excel.

(a) (b)

Figure 3.1: Setup additions.

The additional items were (a) KI Tools interface connected to the current monitor and (b) the modified stainless-steel cathode.

3.3 Data Taking Procedures

Using KI Tools assisted with measuring and plotting the current as it changed over time. Recording the distance traveled during the etching process was done by observing the micrometer throughout the process.

The same procedures as before were followed to form the wire to be etched, and to take data during the procedures. Here, the etching process was concluded when the etching

controller triggered its “Overloaded” feature. This feature meant that the current through the system had been interrupted (dropped to 0 mA) and the controller halted the etching process. The etches that were processed were at shallow depths, so the entire etching process would last around 30 minutes: 15 minutes the wire spent plunging into the solution, then a maximum of 15 minutes (or shorter if the process ended before then) for the wire to be drawn out from the solution.

With the new equipment addition of the KI Tools recording the current, the methods did not change. Having the device reading the current before the process provided a double check and plotted what the current monitor read on the etching controller.

Using the PAX-it! software extra measurements could be taken. Each tip was imaged 4 times at 90-degree rotation intervals about the wire axis (still using the same magnification of 5x). Three separate trials were performed for each inserted depth. In addition to the cone length (mm), Radius A (mm) and Radius B (mm) were measured (see Fig. 1.3). For each tip that was measured at a certain depth, an average value for each variable is calculated, then an averaged 2-D representation was given. This led to being able to calculate the radius of curvature (RoC).

3.4 Results

Table 3.1: Average Values for Tungsten Needle Profile

Averaged Runs	Average RoC (mm)	Average Cone Length (mm)	Average Radius A (mm)	Average Radius B (mm)
1	0.0191	0.3327	0.0504	0.1430
2	0.0017	0.3428	0.0069	0.0291
3	0.0018	0.4879	0.0102	0.0599

(table continues)

Averaged Runs	Average RoC (mm)	Average Cone Length (mm)	Average Radius A (mm)	Average Radius B (mm)
4	0.0021	0.5019	0.0133	0.0831
5	0.0017	0.5330	0.0104	0.0647
6	0.0014	0.5253	0.0088	0.0562

Table 3.2: Standard Deviation for Each Run's Average Value

Averaged Runs	Average RoC (mm)	Average Cone Length (mm)	Average Radius A (mm)	Average Radius B (mm)
1	0.0065	0.0172	0.0073	0.0403
2	0.0002	0.1493	0.0003	0.0011
3	0.0001	0.07	0.0031	0.0302
4	0.0004	0.0094	0.0026	0.0199
5	0.0001	0.0193	0.001	0.015
6	0.0001	0.0547	0.0008	0.0069

Using Radius A and Radius B for the semi-minor and semi-major axis, respectively, an ellipse could be defined. The elliptical cross-section was then used to calculate the radius of curvature (RoC), which was done by using polar coordinates to calculate the curvature, κ, at the apex of the tip. The curvature was then inverted to give the radius of curvature. The calculation for the curvature is as follows:

$$x = r_b cos\theta \qquad y = r_a sin\theta \qquad \text{(Eq. 3.1)}$$

$$\kappa = \frac{|x'y'' - y'x''|}{(x'^2 + y'^2)^{\frac{3}{2}}} = \frac{1}{RoC} \qquad \text{(Eq. 3.2)}$$

where r_b and r_a are the respected semi-major and semi-minor axes associated with the ellipse, and the derivations of x and y are with respect to θ.

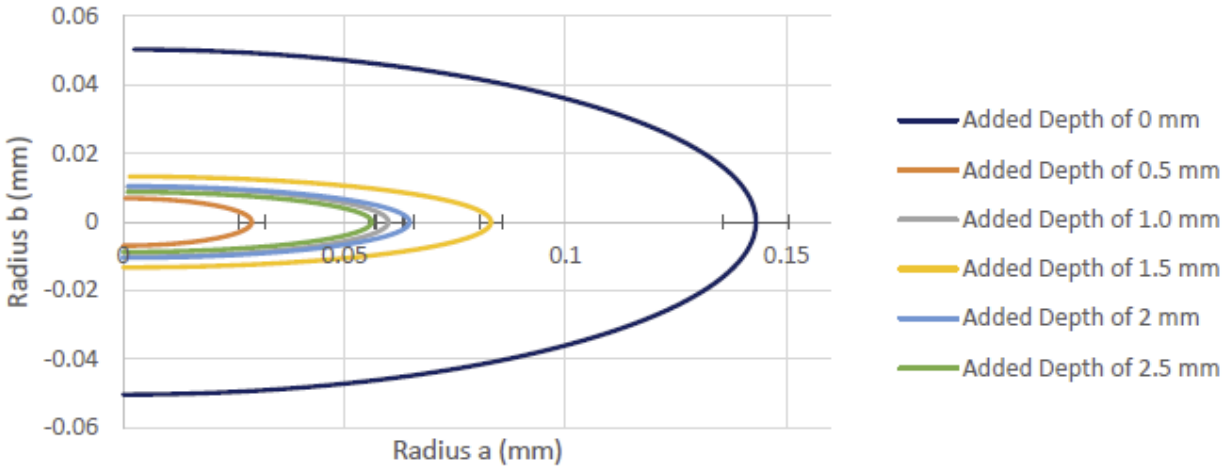

Figure 3.2: Mapped ellipse of cone apex.

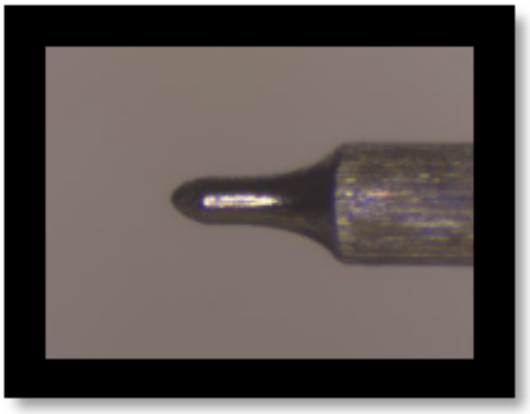

Figure 3.3: Needle profile result at 0.0 mm added depth

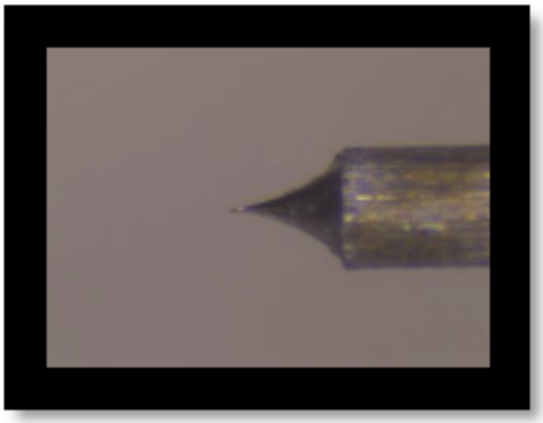

Figure 3.4:Needle profile result at 0.5 mm added depth

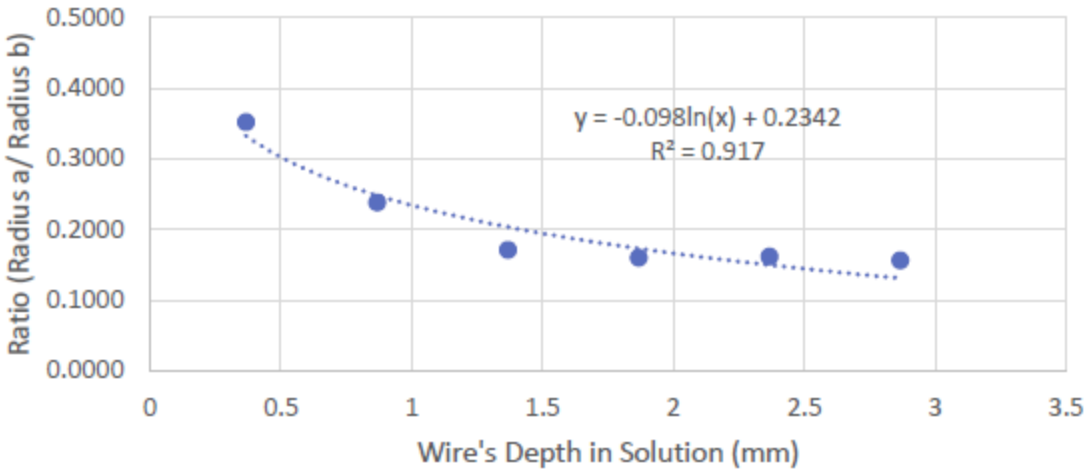

Figure 3.5: Change of elliptical cross-section

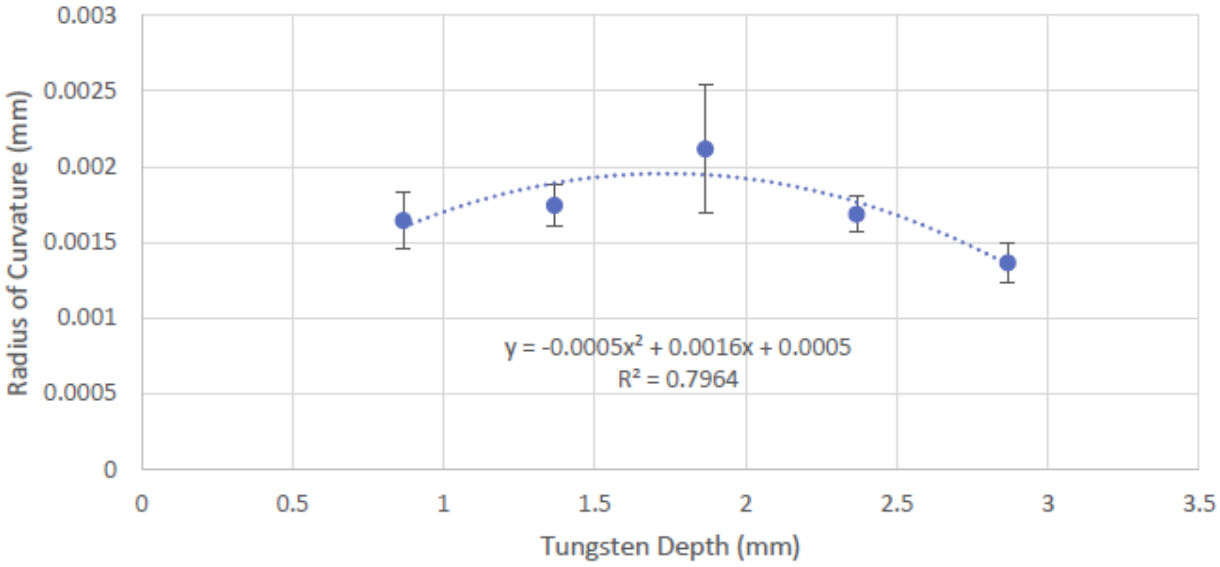

Figure 3.6: RoC vs initial depth

3.5 Discussion

The symmetry of the system improved from the first method setup. The new driver chip provided the system with a much smoother travel, which in turn decreased the amount of mechanical vibration in the tip. When looking at Table 3.2, one sees that the accuracy for each radius increased as the wire was inserted deeper into the solution.

Figures 3.3 and 3.4 show two tip profiles. The initial depth of Figure 3.3 was at 0 mm, while in Figure 3.4, the tip's initial depth was 0.5 mm in the solution. There is an obvious difference between the two tips' profiles. From Table 3.1 it shows that the radius of curvature for the wire inserted at 0 mm is nearly 8 times greater than the wire that was inserted at 0.5 mm. The reason for the dramatic decrease in the radius of curvature (RoC) would be that at the surface of the meniscus there was a decrease in the etching rate due to the OH^- ions concentrated near the surface of the solution [7]. Then, giving the extra depth of 0.5 mm would be enough to break the "barrier" of ions to accelerate the etching rate.

Figure 3.5 shows how as the wire depth was increased; the elliptical cross-section located at the apex of the tip followed a logarithmic trend. A plateau began to emerge as the wire passed a depth of 1 mm into the solution. This implies that the rate at which the tungsten was being etched began to level out and the ability to obtain a consistent elliptical cross-section will increase as the depth is increased.

The trend shown in Figure 3.6 excludes the results obtained from the tungsten wire with the initial depth of 0 mm due to its irregular shape. The tungsten wire, with a starting depth of 0.5 mm, had an accuracy of 64%. This accuracy seemed to increase as the starting depth was pushed further into the solution until a maximum radius of curvature was reached at a depth of around 1.9 mm with an accuracy of 80%. This suggests that around 1.9 mm within the solution, the etching barrier will vary. As the wire was pushed deeper, the accuracy began to increase to 91 – 93 %. As discussed in the previous chapter, one can also see how as the initial depth of the wire is increased then the resulting cone length will also increase with an average replication accuracy of 87% (see Table 3.1).

The hydrogen bubbles emitted from the cathode causes waves to form on the surface of the solution. These waves disturb the shape of the meniscus and can cause the top barrier to alter the etching region. This leads to a tip with an asymmetric needle profile. Lack of symmetry also comes from the end of the wire not being perpendicular to the surface of the solution. This also alters the current level. As bubbles would pop on the surface a sudden spike in the current would be observed. When the current was increased the etching rate was also increased.

3.6 Conclusion

The accuracy of the experiment deviated between a low of 64% to a high of 93% when replicating the curvature of the newly etched tungsten needles.

The symmetric error still poses a problem. Introducing a method to straighten the tungsten wire as its initial depths are very shallow can improve the accuracy of each measured radius in the cone. Having a barrier surrounding the wire shielding it from the bubbles that disturb the surface the solution can avoid any unnecessary spike in current. Operating at lower voltages is an option, however, the integrity of the tip surface would need to be considered.

CHAPTER 4

CONCLUSION

Each experiment had its own focused goal, but it all stemmed from understanding more about the production and replication of the newly etched tungsten needles. These needles would have uses for a range of SPMs and LIMPS studies. This dynamic plunging method is a reliable technique for obtaining various curvatures and cone lengths needed for these studies. Using the combination of etching tips near the surface of the solution and having the wire staying within the etching barrier provided sharp tips that are reproducible to a high accuracy.

APPENDIX

ARDUINO UNO R3 “PLUNGING” CODE

The code that is below was constructed from the Arduino IDE interface. It was programmed to set the delay speed of the stepping motor and would change the direction of the wire as it passed throughout the solution.

```
#include <Stepper.h>

// defines pins numbers
  const int stepPin = 3;
  const int dirPin = 4;
  const int enablePin = 2;
  const int tgPin7 = 7; //Toggle for ON
  const int tgPin8 = 8; //Toggle for ON
  int statePin7;
  int statePin8;

  int steps = 0;
  float lsteps = steps; // Long form of steps for calculations

  float initspeed = 0.26381147;                    // Initial speed,
unmodified, in steps/second
  float accelerat = 0.00009666;                    // Acceleration,
unmodified, in steps/second^2
  float minitsped = 0.99926844;                    // Modification of
speed, slope value
  float binitsped = 0.00007738;                    // Modification of
speed, constant value
  float maccelert = 1.00048765;                    // Modification of
acceleration, slope value
  float baccelert = 0.00000002;                    // Modification of
acceleration, constant value
  float realspeed = minitsped*initspeed+binitsped; // Modified speed
for use in constant speed calc
  float realaccel = maccelert*accelerat+baccelert; // Modified
acceleration for use in constant speed calc

// Speed as a function of time          :: a*t + v0
// Time as a function of steps          ::
(v0/a)*((2*a*steps/v0/v0+1)^1/2-1)
// Modified speed as a function of time :: a'*t + v0' =
(m_a*a+b_a)*t+(m_v*v0+b_v)
// Modified speed as a function of step ::
(m_a*a+b_a)*(v0/a)*((2*a*steps/v0/v0+1)^1/2-1)+(m_v*v0+b_v)
// Modified time as a function of steps ::
1/((m_a*a+b_a)*(v0/a)*((2*a*steps/v0/v0+1)^1/2-1)+(m_v*v0+b_v))

  float spdfxnstp =
(float)(realaccel*(initspeed/accelerat)*(sqrt(2.0*accelerat*lsteps/pow
(initspeed,2.0)+1.0)-1.0)+realspeed);
```

```
  long timfxnstp = round(1/(spdfxnstp/1000));

  unsigned long start, finish, elapse, total;     // Timing for
printing trial time

void setup()
{
  // Sets the 3 pins as Outputs
  pinMode(stepPin,OUTPUT);
  pinMode(dirPin,OUTPUT);
  pinMode(enablePin,OUTPUT);
  pinMode(tgPin7,INPUT);
  pinMode(tgPin8,INPUT);

  Serial.begin(115200);
  Serial.println("Stepper Micrometer");

  Serial.print("INITSPEED");
  Serial.print("\t");

  Serial.print("ACCELERAT");
  Serial.print("\t");

  Serial.print("MINITSPED");
  Serial.print("\t");

  Serial.print("BINITSPED");
  Serial.print("\t");

  Serial.print("MACCELERT");
  Serial.print("\t");

  Serial.print("BACCELERT");
  Serial.print("\t");

  Serial.print("REALSPEED");
  Serial.print("\t");

  Serial.println("REALACCEL");

  Serial.print(initspeed,8);
  Serial.print("\t");

  Serial.print(accelerat,8);
  Serial.print("\t");

  Serial.print(minitsped,8);
  Serial.print("\t");

  Serial.print(binitsped,8);
  Serial.print("\t");
```

```
  Serial.print(maccelert,8);
  Serial.print("\t");

  Serial.print(baccelert,8);
  Serial.print("\t");

  Serial.print(realspeed,8);
  Serial.print("\t");

  Serial.println(realaccel,8);

  Serial.print("NUM_STEPS");
  Serial.print("\t");

  Serial.print("SPDFXNSTP");
  Serial.print("\t");

  Serial.print("ELAPSED_T");
  Serial.print("\t");

  Serial.println("TOTAL_mT");
}
void loop()
{
  statePin7 = digitalRead(tgPin7);
  statePin8 = digitalRead(tgPin8);

  if(statePin7 == HIGH && statePin8 == LOW) // Switch is ON (sending
5V to pin 7)
  {
    digitalWrite(enablePin,LOW);
    digitalWrite(dirPin,HIGH); // Enables the motor to move in a
particular direction
    digitalWrite(stepPin,HIGH);

    start = millis();

    steps++;
    lsteps = steps;
    spdfxnstp =
(float)(realaccel*(initspeed/accelerat)*(sqrt(2.0*accelerat*lsteps/pow
(initspeed,2.0)+1.0)-1.0)+realspeed);
    timfxnstp = round(1/(spdfxnstp/1000));

    delay(0.98*timfxnstp);

    finish = millis();
    elapse = finish-start;
    total = total+elapse;

    Serial.print(lsteps,0);
    Serial.print("\t");
```

```
    Serial.print("\t");

    Serial.print(spdfxnstp,8);
    Serial.print("\t");

    Serial.print(elapse);
    Serial.print("\t");
    Serial.print("\t");

    Serial.println(total);
  }
  else if(statePin8 == HIGH && statePin7 == LOW) // Switch is ON
(sending 5V to pin 8)
  {
    digitalWrite(enablePin,LOW);
    digitalWrite(dirPin,LOW); //Changes the rotations direction
    digitalWrite(stepPin,HIGH);

    start = millis();

    steps++;
    lsteps = steps;
    spdfxnstp =
(float)(realaccel*(initspeed/accelerat)*(sqrt(2.0*accelerat*lsteps/pow
(initspeed,2.0)+1.0)-1.0)+realspeed);
    timfxnstp = round(1/(spdfxnstp/1000));

    delay(0.98*timfxnstp);

    finish = millis();
    elapse = finish-start;
    total = total+elapse;

    Serial.print(lsteps,0);
    Serial.print("\t");
    Serial.print("\t");

    Serial.print(spdfxnstp,8);
    Serial.print("\t");

    Serial.print(elapse);
    Serial.print("\t");
    Serial.print("\t");

    Serial.println(total);
  }
  else
  {
    digitalWrite(enablePin,HIGH); // Switch is OFF and stops the
motion of the motor
  }
}
```

REFERENCES

[1] Mair, G L, and R G Forbes. “Analytical Determination of the Dimensions and Evolution with Current of the Ion-Emitting Jet in Liquid-Metal Ion Sources.” *Journal of Physics D: Applied Physics*, vol. 24, no. 12, 1991, pp. 2217–2221., doi:10.1088/0022-3727/24/12/014.

[2] Kim, Pilkyu, et al. “Efficient Electrochemical Etching Method to Fabricate Sharp Metallic Tips for Scanning Probe Microscopes.” *Review of Scientific Instruments*, vol. 77, no. 10, 11 Oct. 2006, pp. 103706–1-103706–5., doi:10.1063/1.2358703.

[3] Czarczynski, Wojciech, and Zbigniew Znamirowski. “Liquid Metal Ion Sources.” *Vacuum*, vol. 44, no. 11-12, 1993, pp. 1095–1099., doi:10.1016/0042-207x(93)90330-d.

[4] Chang, Wei-Tse, et al. “Method of Electrochemical Etching of Tungsten Tips with Controllable Profiles.” *Review of Scientific Instruments*, vol. 83, no. 8, 15 Aug. 2012, p. 083704., doi:10.1063/1.4745394.

[5] Ibe, J. P., et al. “On the Electrochemical Etching of Tips for Scanning Tunneling Microscopy.” *Journal of Vacuum Science & Technology A: Vacuum, Surfaces, and Films*, vol. 8, no. 4, 1990, pp. 3570–3575., doi:10.1116/1.576509.

[6] Ju, Bing-Feng, et al. “The Art of Electrochemical Etching for Preparing Tungsten Probes with Controllable Tip Profile and Characteristic Parameters.” *Review of Scientific Instruments*, vol. 82, no. 1, 28 Jan. 2011, pp. 013707–1-013707–8., doi:10.1063/1.3529880.

[7] Basnet, Gobind, "Fabrication of Tungsten Tips Suitable for Scanning Probe Microscopy by Electrochemical Etching Methods" (2013). *Theses and Dissertations*. 865. http://scholarworks.uark.edu/etd/865

[8] Guo, Dengshuai, et al. “Note: Fabrication of Roughened Tips for Liquid Metal Ion Sources.” *Review of Scientific Instruments*, vol. 88, no. 6, 27 June 2017, p. 066107., doi:10.1063/1.4985635.